Chinese Chemical Letters 33 (2022) 4700–4704

Contents lists available at ScienceDirect

Chinese Chemical Letters

journal homepage: www.elsevier.com/locate/cclet

Construction of high-efficiency CoS@Nb_2O_5 heterojunctions accelerating charge transfer for boosting photocatalytic hydrogen evolution

Xin Ren[a,b,1], Jianyou Shi[c,1], Ruihuan Duan[d,1], Jun Di[d], Chao Xue[e], Xiao Luo[f], Qing Liu[f], Mengyang Xia[b,*], Bo Lin[b,*], Wu Tang[a,*]

[a] School of Materials and Energy, University of Electronic Science and Technology of China, Chengdu 611731, China
[b] XJTU-Oxford International Joint Laboratory for Catalysis, School of Chemical Engineering and Technology, Xi'an Jiaotong University, Xi'an 710049, China
[c] Personalized Drug Therapy Key Laboratory of Sichuan Province, Sichuan Academy of Medical Science & Sichuan Provincial People's Hospital, School of Medicine, University of Electronic Science and Technology of China, Chengdu 610072, China
[d] School of Materials Science and Engineering, Nanyang Technological University, 639798, Singapore
[e] State Centre for International Cooperation on Designer Low-carbon and Environmental Materials (CDLCEM), School of Materials Science and Engineering, Zhengzhou University, Zhengzhou 450001, China
[f] School of Optoelectronic Science and Engineering, University of Electronic Science and Technology of China, Chengdu 611731, China

ARTICLE INFO

Article history:
Received 18 October 2021
Revised 12 November 2021
Accepted 27 December 2021
Available online 2 January 2022

Keywords:
Transition metal chalcogenides
CoS cocatalyst
Nb_2O_5 nanosheets
Charge transfer
Photocatalytic H_2 evolution

ABSTRACT

The random movement and easy recombination of photoinduced charges lead to a low conversion efficiency for photocatalytic hydrogen evolution. The cocatalyst design is a promising route to address such problem through introducing an appropriate cocatalyst on the semiconductor photocatalysts to construct the high-efficiency heterojunctions. Herein, novel CoS/Nb_2O_5 heterojunctions were constructed *via in-situ* loading CoS cocatalyst on the surface of Nb_2O_5 nanosheets. Through the femtosecond-resolved transient absorption spectroscopy, the average lifetime of charge carriers for 10 wt% CoS/Nb_2O_5 (159.6 ps) is drastically shortened by contrast with that of Nb_2O_5 (5531.9 ps), strongly suggesting the rapid charge transfer from Nb_2O_5 to CoS. The significantly improved charge-transfer capacity contributes to a high photocatalytic hydrogen evolution rate of 355 μmol/h, up to 17.5 times compared with pristine Nb_2O_5. This work would provide a new design platform in the construction of photocatalytic heterojunctions with high charge-transfer efficiency.

Photocatalytic water splitting driven by the solar energy for hydrogen generation is regarded as an efficient strategy to address the global energy crisis [1,2]. The entire photocatalytic reaction can be roughly divided into 3 steps including light capture, charge separation and migration, and redox reactions at the active sites on the surface of photocatalysts [3,4]. It is worth noting that the easy recombination of photogenerated carriers during the charge separation and transfer process can result in the low conversion efficiency of photocatalytic hydrogen evolution [5–7]. One effective route to address such challenge is the loading of appropriate cocatalysts on the surface of photocatalysts to construct heterojunctions, which can introduce more active sites and transfer paths for charges, thus achieving high-efficiency charge separation and transfer during the photocatalytic reaction [8–10]. The widely used cocatalysts for photocatalytic hydrogen evolution are noble metals such as platinum (Pt) and Aurum (Au) owing to their superior photocatalytic activity and chemical stability. However, the scarcity and high utilization cost significantly limit their practical applications [11–13]. Therefore, it is of vital importance to seek the alternative cocatalysts with both excellent catalytic performance and low operating cost.

Recently, transition metal chalcogenides (shorted for TMCs) such as CdS [14], ZnS [15,16], $ZnIn_2S_4$ [6,17], WS_2 [18], MoS_2 [19,20] and NiS [21], have triggered keen interest due to their suitable band gap, outstanding light harvesting, low cost, which enable TMCs to be the promising cocatalysts in photocatalytic hydrogen evolution [22–24]. Among the TMCs group, CoS possesses many favorable advantages, including narrow bandgap, low toxicity and excellent conductivity, which allows it to be an ideal

* Corresponding authors.
E-mail addresses: nearsoul@stu.xjtu.edu.cn (M. Xia), bolinscet@xjtu.edu.cn (B. Lin), tang@uestc.edu.cn (W. Tang).
[1] These authors contributed equally to this work.

https://doi.org/10.1016/j.cclet.2021.12.076
1001-8417/

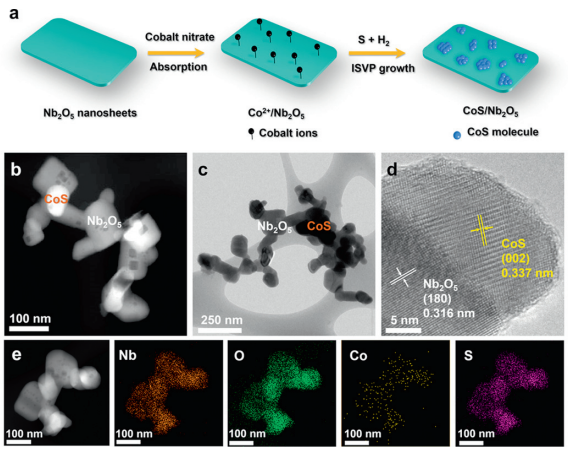

Fig. 1. (a) Schematic illustration of the synthesis of CoS/Nb_2O_5. (b) HAADF-STEM (c) TEM and (d) HRTEM images of CoS/Nb_2O_5. (e) HAADF-STEM and elemental mapping images of CoS/Nb_2O_5.

cocatalyst in the design of binary photocatalytic system for H_2 evolution [25–27].

Herein, we report an efficient CoS/Nb_2O_5 heterostructured photocatalyst *via* a one-step *in-situ* vapor-phase growth method, where the CoS cocatalyst *in-situ* grew on the surface of Nb_2O_5 nanosheets with the advantages of outstanding photocatalytic H_2 evolution activity. Under the synergistic effects of heterojunction and CoS cocatalyst, the charge-transfer efficiency of CoS/Nb_2O_5 is boosted significantly, thus leading to a high hydrogen evolution rate (HER) of 355 μmol/h, up to 17.5 times compared with pristine Nb_2O_5 nanosheets.

The CoS/Nb_2O_5 heterojunctions were synthesized using an *in-situ* vapor-phase growth method (shorted for ISVP). As shown in Fig. 1a, Nb_2O_5 nanosheet was synthesized through a template-assisted calcination method according to the previous report [28]. Then the Nb_2O_5 nanosheet was dispersed into an aqueous solution with a certain amount of cobalt nitrate hexahydrate, where cobalt ions anchored on the surface of Nb_2O_5 nanosheets to obtain Co^{2+}/Nb_2O_5. After that, the Co^{2+}/Nb_2O_5 were heated to 700 °C with pure sulfur powder simultaneously in a mixed atmosphere (20% H_2 and 80% Ar). Under high-temperature environment, sulfur powder firstly reacted with H_2 to form H_2S, then H_2S can reduce the cobalt nitrate absorbed on the surface of Nb_2O_5 to form the CoS nanoparticles, thus obtaining the CoS/Nb_2O_5 heterojunctions. The morphology of CoS/Nb_2O_5 was investigated by transmission electron microscopy (TEM) and high-angle annular dark-field scanning transmission electron microscopy (HAADF-STEM). As shown in Figs. 1b and c, some well-dispersed CoS nanoparticles were loaded on the surface of Nb_2O_5 nanosheets with an average length of 50 nm and a width of 50 nm. Furthermore, the high-resolution TEM (HRTEM) image further reveals the detail of interface structure of CoS/Nb_2O_5. As displayed in Fig. 1d, the adjacent lattice-fringe spacings of 0.316 and 0.337 nm corresponded to the (180) reflection plane of Nb_2O_5 and the (002) reflection plane of CoS respectively [29,30], which strongly supports the successful construction of the CoS/Nb_2O_5 heterojunctions. Additionally, the elemental mapping (Fig. 1e) and energy-dispersive X-ray spectroscopy (EDX) images (Fig. S1 in Supporting information) further confirm the successful construction of CoS/Nb_2O_5 heterojunction photocatalyst.

To explore the crystallinity of Nb_2O_5 and CoS, the X-ray diffraction (XRD) patterns of 10 wt% CoS/Nb_2O_5 and Nb_2O_5 were carried out. As shown in Fig. 2a, all diffraction peaks of Nb_2O_5 well fit the orthorhombic crystalline state (JCPDS No. 30–0873). For the XRD pattern of 10 wt% CoS/Nb_2O_5, three low-intensity peaks at 30.6°, 35.3°and 46.9° are in accord with the hexagonal phase of CoS (JCPDS No. 65–3418) [31], while the peaks around 25° ∼ 28° correspond to a slight amount of cobalt sulfate (JCPDS No. 15–0701) on the surface of CoS/Nb_2O_5 sample. Additionally, all other XRD peaks are corresponded to the orthorhombic crystalline state of Nb_2O_5. The X-ray photoelectron spectroscopy (XPS) was carried out to further analyze the surface chemical state and element composition of Nb_2O_5 nanosheet and 10 wt% CoS/Nb_2O_5. As displayed in Fig. 2b and Fig. S2 (Supporting information), the XPS spectra of both samples show the similar peaks of Nb and O elements. Besides, the peaks of S and Co elements occurred in XPS spectra of 10 wt% CoS/Nb_2O_5, indicating the successful loading of CoS on the surface of Nb_2O_5. In Fig. 2c, the spectrum of Co 2p region has four distinct diffraction peaks, the peaks at 782.33 and 785.95 eV are attributed to Co $2p_{3/2}$, while the peak at 798.44 and 802.83 eV corresponded to Co $2p_{1/2}$ [32,33]. In Fig. 2d, the peaks at 207.65 and 210.39 eV are ascribed to Nb $3d_{5/2}$ and Nb $3d_{3/2}$ in Nb_2O_5 nanosheets, respectively [34]. As exhibited in Fig. 2e, the peaks at 169.6 and 171.13 eV are attributed to S $2p_{3/2}$ and S $2p_{1/2}$, which are related to the amorphous phases of CoS [35]. In Fig. 2f, the peak at 530.49 eV is corresponded to Nb−O bond, the other two peaks at 533.57 and 532.53 eV are associated with physically adsorbed water molecules and oxygen from the precursor of niobium [36,37]. The XRD and XPS results presented above strongly demonstrated the successful construction of the CoS/Nb_2O_5 heterostructured photocatalyst. The construction of efficient heterojunction can increase the charge separation and transfer efficiency significantly, thus boosting photocatalytic hydrogen evolution activity [38].

Time-dependent photocatalytic H_2 production experiments over Nb_2O_5 and CoS/Nb_2O_5 samples were evaluated under the simulated solar-light irradiation ($\lambda \geq 300$ nm) with triethanolamine (TEOA) as the hole-scavenger. As shown in Fig. 3a, pristine Nb_2O_5 exhibits a poor hydrogen evolution rate of average 20.3 μmol/h, indicating its inferior charge-transfer capacity. However, it can be observed that the CoS/Nb_2O_5 with the optimal cocatalyst-loading amount (10 wt%, Fig. S3 in Supporting information) shows a high HER of 355 μmol/h, up to 17.5 times compared with pristine Nb_2O_5, strongly demonstrating the advantages of the CoS/Nb_2O_5 heterostructure. The apparent quantum efficiency (AQE) of 10 wt% CoS/Nb_2O_5 was evaluated and estimated to be 5.93% at 365 nm (Table S1 in Supporting information), exceeding most of wide-band-gap photocatalysts such as TiO_2 and some composite photocatalysts [18,39–42]. The cycling stability of hydrogen production over CoS/Nb_2O_5 was evaluated. As displayed in Fig. 3b, after 4 cycling tests, 10 wt% CoS/Nb_2O_5 still exhibits an excellent H_2 evolution rate, only 9.4% decay was observed. Besides, the TEM and HAADF-STEM images of 10 wt% CoS/Nb_2O_5 after 4 cycling tests also well support its excellent stability. As shown in Fig. S4 (Supporting information), CoS/Nb_2O_5 still maintain a relatively intact stable heterostructure, as evidenced by the elemental mappings image (Fig. S4d). Additionally, the XRD pattern of recycled 10 wt% CoS/Nb_2O_5 (Fig. S5 in Supporting information) shows a similar trend by contrast with fresh 10 wt% CoS/Nb_2O_5, further confirming its stability.

To investigate the major factors for the excellent photocatalytic activity of 10 wt% CoS/Nb_2O_5, various properties of the synthesized samples including optics, texture and photoelectricity were studied. The UV-vis diffuse reflectance spectra (DRS) of Nb_2O_5 and 10 wt% CoS/Nb_2O_5 are carried out. As displayed in Fig. 4a, Nb_2O_5 has a routine light absorption in the ultraviolet region ($\leq$ 400 nm), which corresponded to the calculated band-gap energy (E_g) of 3.1 eV. However, with the construction of the binary heterojunction, the light absorption capacity of 10 wt% CoS/Nb_2O_5 was greatly enhanced whether in the ultraviolet and visible regions, which is mainly due to the effect of CoS [43]. Besides, as shown in Fig. S6 (Supporting information), compared to Nb_2O_5 sample, the color of 10 wt% CoS/Nb_2O_5 sample changed from white

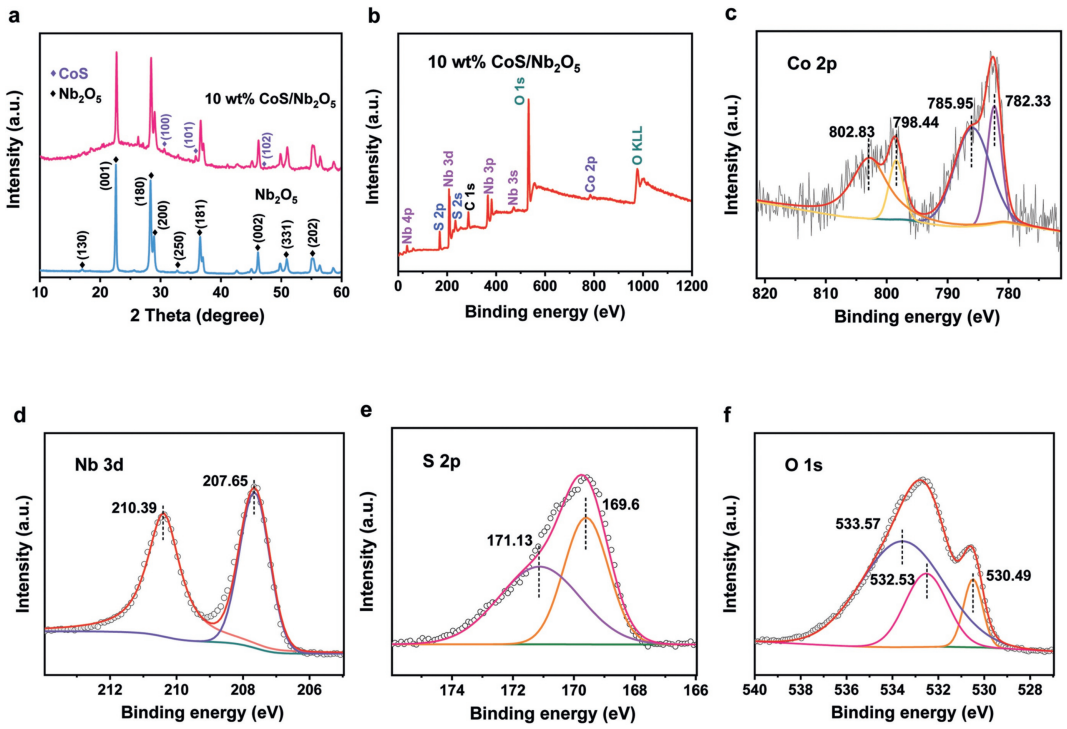

Fig. 2. (a) XRD patterns of Nb_2O_5 and 10 wt% CoS/Nb_2O_5. (b) XPS patterns full spectrum of 10 wt% CoS/Nb_2O_5 and its corresponding regions of (c) Co 2p, (d) Nb 3d, (e) S 2p, (f) O 1s.

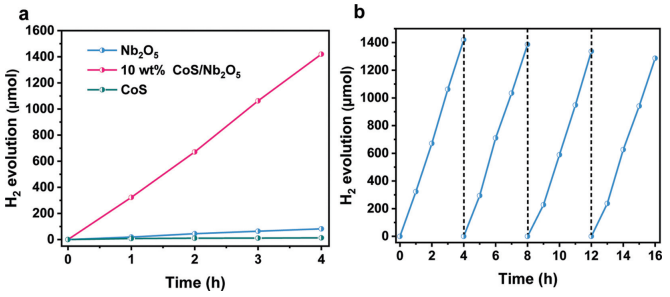

Fig. 3. (a) Time-dependent photocatalytic H_2 evolution of Nb_2O_5 and 10 wt% CoS/Nb_2O_5 under solar-light irradiation ($\lambda \geq 300$ nm). (b) Cycling H_2 evolution tests of 10 wt% CoS/Nb_2O_5 under solar-light irradiation ($\lambda \geq 300$ nm).

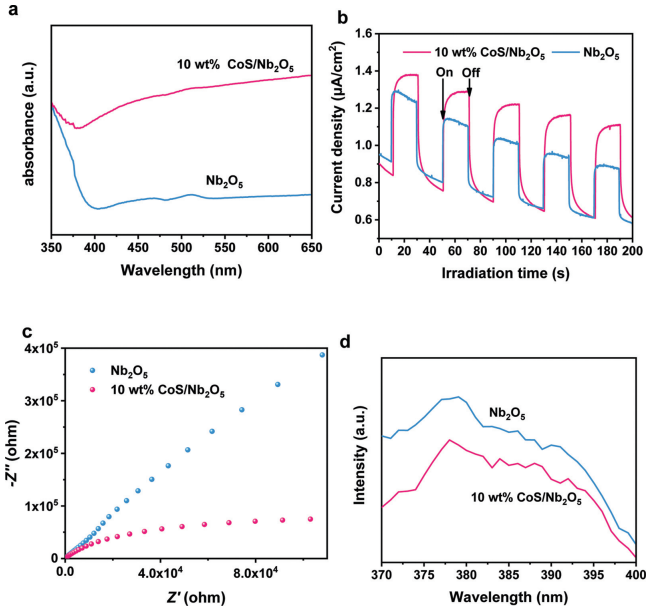

Fig. 4. (a) UV-vis diffuse reflectance spectra of Nb_2O_5 and 10 wt% CoS/Nb_2O_5. (b) Transient photocurrent responses of Nb_2O_5 and 10 wt% CoS/Nb_2O_5. (c) Electrochemical impedance spectroscopy Nyquist plots of Nb_2O_5 and 10 wt% CoS/Nb_2O_5. (d) Photoluminescence spectra of Nb_2O_5 and 10 wt% CoS/Nb_2O_5.

to gray, indicating the variation in photo-absorption. The specific textural information of Nb_2O_5 and 10 wt% CoS/Nb_2O_5 is listed in Table S2 (Supporting information). As shown in Table S2, 10 wt% CoS/Nb_2O_5 possesses a higher specific surface (9.31 m^2/g) and pore volume (0.04 cm^3/g) compared with pristine Nb_2O_5 (7.84 m^2/g and 0.03 cm^3/g, respectively), which is beneficial to the photocatalytic H_2 evolution by introducing more reaction active sites [44].

To investigate the charge separation and transfer capacity of Nb_2O_5 and 10 wt% CoS/Nb_2O_5, transient photocurrent responses, electrochemical impedance spectroscopy (EIS) and photoluminescence (PL) spectra were carried out. As exhibited in Fig. 4b, 10 wt% CoS/Nb_2O_5 displays a higher transient photocurrent density than Nb_2O_5, indicating the superior charge transfer efficiency [45]. Besides, the EIS spectra (Fig. 4c) show that 10 wt% CoS/Nb_2O_5 displays a smaller radius of Nyquist circle by contrast with pristine Nb_2O_5, which strongly prove the minimum charge transfer obstruction of 10 wt% CoS/Nb_2O_5. Photoluminescence spectrum (PL) is an important characterization to study the separation and recombination of photogenerated charges, which is closely connected to the photocatalytic process. As the PL spectra shown in Fig. 4d, a lower emission peak intensity was observed of 10 wt% CoS/Nb_2O_5 by contrast with pristine Nb_2O_5. This result indicates that the suppressive recombination of charges leads to the reduced energy released in the form of PL. Therefore, more charges in CoS/Nb_2O_5 system can participate in the photocatalytic reaction, thus achieving a high hydrogen evolution rate of 355 μmol/h [46–49].

Furthermore, femtosecond-resolved transient absorption spectroscopy (TAS) is powerful technique for investigating the separa-

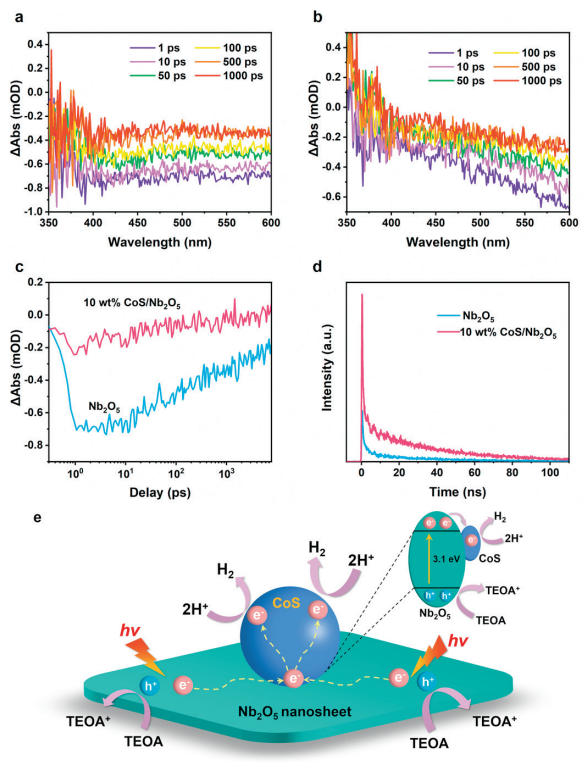

Fig. 5. Femtosecond-resolved TAS spectra of (a) Nb_2O_5 and (b) 10 wt% CoS/Nb_2O_5. (c) TAS kinetics probed at 360 to 420 nm for Nb_2O_5 and 10 wt% CoS/Nb_2O_5. (d) Time-resolved fluorescence decay spectra of Nb_2O_5 and 10 wt% CoS/Nb_2O_5. (e) The schematic of charge transfer in the CoS/Nb_2O_5 system for photocatalytic H_2 evolution.

tion and transfer of charges. As displayed in Figs. 5a and b, the specific-time-points TAS spectra from 1 ps to 1000 ps of Nb_2O_5 and 10 wt% CoS/Nb_2O_5 are marked with different colors. Both Nb_2O_5 and 10 wt% CoS/Nb_2O_5 exhibit a broad negative induced absorption, which are attributed to the effect of overlapping electron and hole absorption in Nb_2O_5 [50–52]. The kinetics of TAS from 360 nm to 420 nm (Fig. 5c) of Nb_2O_5 and 10 wt% CoS/Nb_2O_5 is investigated to reveal the lifetime of charge carriers. As shown in Table S3 (Supporting information), by fitting the kinetics curve with two-exponential decay functions, the average lifetime of charge carriers for 10 wt% CoS/Nb_2O_5 is 159.6 ps, which is far lower than that of Nb_2O_5 (5531.9 ps). The considerably shorted lifetime strongly indicates the rapid charge transfer from Nb_2O_5 to CoS, which is in accord with the time-resolved fluorescence decay spectra results (Fig. 5d and Table S4 in Supporting information) [50,53].

According to all the characterization and analytical results presented above, a probable mechanism for the charge transfer in photocatalytic hydrogen evolution of CoS/Nb_2O_5 photocatalyst has been proposed. As illustrated in Fig. 5e, Nb_2O_5 nanosheets in the CoS/Nb_2O_5 system can be excited to generate numerous photoinduced electron-hole pairs under the simulated solar-light irradiation ($\lambda \geq 300$ nm). The photoinduced electrons are rapidly injected into its conduction band (CB), while the photoinduced holes that remained in the valence band (VB) are captured by the hole-scavenger of triethanolamine (TEOA). Owing to the construction of the binary CoS/Nb_2O_5 system, the photoinduced electrons on the Nb_2O_5 nanosheets can rapidly transfer to CoS with abundant active sites *via* the heterojunction interfaces. Then the electrons reduce hydrogen ions in aqueous solution into H_2 at the active sites on the surface of CoS cocatalyst [54–56]. The significantly accelerated charge transfer contributes to the excellent photocatalytic H_2 evolution activity of 10 wt% CoS/Nb_2O_5.

In summary, the high-efficiency CoS/Nb_2O_5 heterojunctions were successfully synthesized through a one-step vapor growth method. Taking advantage of the advanced femtosecond-resolved ultrafast TAS spectra, we reveal that the average lifetime of charge carriers for 10 wt% CoS/Nb_2O_5 (159.6 ps) is drastically shortened by contrast with that of Nb_2O_5 (5531.9 ps), strongly suggesting the rapid charge transfer from Nb_2O_5 to CoS. The improved charge transfer efficiency leads to a high photocatalytic H_2 evolution of 355 μmol/h, up to 17.5 times by contrast with pure Nb_2O_5.

Declaration of competing interest

The authors declare no conflict of competing interest.

Acknowledgments

This work was funded by the National Natural Science Foundation of China (No. 22002014), Applied Basic Research Program of Sichuan Province (No. 2020YJ0068), "Young Talent Support Plan" of Xi'an Jiaotong University, National Key Research and Development Program of China (No. 2020YFC2005500), Key Research and Development Program of Science and Technology Department of Sichuan Province (No. 2019YFS0514). Dr. Chao Xue acknowledges financial support from the National Natural Science Foundation of China (No. 22102152).

Supplementary materials

Supplementary material associated with this article can be found, in the online version, at doi:10.1016/j.cclet.2021.12.076.

References

[1] B. Dai, J. Fang, Y. Yu, et al., Adv. Mater. 32 (2020) 1906361.
[2] Y. Wang, H. Suzuki, J. Xie, et al., Chem. Rev. 118 (2018) 5201–5241.
[3] T.A. Pham, Y. Ping, G. Galli, Nat. Mater. 16 (2017) 401–408.
[4] F. Liu, N. Feng, Q. Wang, et al., J. Am. Chem. Soc. 139 (2017) 10020–10028.
[5] X. Jin, R. Wang, L. Zhang, et al., Angew. Chem. Int. Ed. 132 (2020) 6894–6898.
[6] B. Lin, H. Li, H. An, et al., Appl. Catal. B: Environ. 220 (2018) 542–552.
[7] B. Lin, A. Chaturvedi, J. Di, et al., Nano Energy 76 (2020) 104972.
[8] M. Liu, Y. Chen, J. Su, et al., Nat. Energy 1 (2016) 16151.
[9] D. Gao, B. Zhao, F. Chen, et al., ACS Sustain. Chem. Eng. 9 (2021) 8653–8662.
[10] R. Wei, Z. Huang, G. Gu, et al., Appl. Catal. B: Environ. 231 (2018) 101–107.
[11] C. Wang, K. Wang, Y. Feng, et al., Adv. Mater. 33 (2021) 2003327.
[12] R. Shen, K. He, A. Zhang, et al., Appl. Catal. B: Environ. 291 (2021) 120104.
[13] N. Zheng, T. Ouyang, Y. Chen, et al., Catal. Sci. Technol. 9 (2019) 1357–1364.
[14] R. Shen, D. Ren, Y. Ding, et al., Sci. China Mater. 63 (2020) 2153–2188.
[15] X. Hao, J. Zhou, Z. Cui, et al., Appl. Catal. B: Environ. 229 (2018) 41–51.
[16] Z. Dong, Y. Wu, N. Thirugnanam, G. Li, Appl. Surf. Sci. 430 (2018) 293–300.
[17] G. Zuo, Y. Wang, W.L. Teo, et al., Angew. Chem. Int. Ed. 132 (2020) 11383–11388.
[18] B. Lin, H. Chen, Y. Zhou, et al., Chin. Chem. Lett. 32 (2021) 3128–3132.
[19] Z. Liang, R. Shen, Y.H. Ng, et al., J. Mater. Sci. Technol. 56 (2020) 89–121.
[20] X. Shi, M. Fujitsuka, S. Kim, T. Majima, Small 14 (2018) 1703277.
[21] L. Zhang, X. Hao, Y. Li, Z. Jin, Appl. Surf. Sci. 499 (2020) 143862.
[22] Q. Lu, Y. Yu, Q. Ma, B. Chen, H. Zhang, Adv. Mater. 28 (2016) 1917–1933.
[23] F. Haque, T. Daeneke, K. Kalantar-Zadeh, J.Z. Ou, Nano Micro Lett. 10 (2018) 23.
[24] Y. Chen, J. Li, P. Liao, et al., Chin. Chem. Lett. 31 (2020) 1516–1519.
[25] J. Ran, H. Zhang, J. Qu, et al., ACS Mater. Lett. 2 (2020) 1484–1494.
[26] J. Yan, G. Wu, N. Guan, L. Li, Appl. Catal. B Environ. 152-153 (2014) 280–288.
[27] S.M. Lam, J.C. Sin, I. Satoshi, A.Z. Abdullah, A.R. Mohamed, Appl. Catal. A: Gen. 471 (2014) 126–135.
[28] B. Lin, Y. Zhou, B. Xu, et al., Mater. Horiz. 8 (2021) 612–618.
[29] B. Lin, Z. Chen, P. Song, et al., Small 16 (2020) 2003302.
[30] Y. Chen, X. Li, K. Park, et al., Angew. Chem. Int. Ed. 55 (2016) 15831–15834.
[31] D. He, D. Wu, J. Gao, et al., J. Power Sources 294 (2015) 643–649.
[32] G. Ai, R. Mo, H. Li, J. Zhong, Nanoscale 7 (2015) 6722–6728.
[33] M. Zhu, L. Zhang, S. Liu, et al., Chin. Chem. Lett. 31 (2020) 1961–1965.
[34] M. Qamar, M. Abdalwadoud, M.I. Ahmed, et al., ACS Appl. Mater. Interfaces 7 (2015) 17954–17962.
[35] Y. Li, J. Xu, Z. Liu, H. Yu, J. Mater. Sci. Mater. Electron. 30 (2019) 246–258.
[36] S. Xiong, J.S. Chen, X.W. Lou, H.C. Zeng, Adv. Funct. Mater. 22 (2012) 861–871.
[37] G.T.S.T. da Silva, K.T.G. Carvalho, O.F. Lopes, C. Ribeiro, Appl. Catal. B: Environ. 216 (2017) 70–79.
[38] C. Cheng, B. He, J. Fan, et al., Adv. Mater. 33 (2021) 2100317.
[39] F. He, A. Meng, B. Cheng, W. Ho, J. Yu, Chin. J. Catal. 41 (2020) 9–20.
[40] Z. Zhang, K. Liu, Y. Bao, B. Dong, Appl. Catal. B: Environ. 203 (2017) 599–606.

[41] J. Yan, H. Wu, H. Chen, et al., Appl. Catal. B: Environ. 191 (2016) 130–137.
[42] H. Li, P. Wang, X. Yi, H. Yu, Appl. Catal. B: Environ. 264 (2020) 118504.
[43] Y. Liu, X. Zhang, Y. Wang, et al., Int. J. Hydrog. Energy 44 (2019) 17697–17708.
[44] G. Jia, Y. Wang, X. Cui, et al., Appl. Catal. B: Environ. 258 (2019) 117959.
[45] D. Gao, J. Xu, H. Yu, Y. Liu, J. Yu, Chem. Commun. 57 (2021) 2025–2028.
[46] T. Su, R. Peng, Z.D. Hood, et al., ChemSusChem 11 (2018) 688–699.
[47] L. Ye, X. Jin, X. Ji, et al., Chem. Eng. J. 291 (2016) 39–46.
[48] X. Jiang, L. Zhang, H. Liu, et al., Angew. Chem. Int. Ed. 132 (2020) 23112–23116.
[49] L. Zheng, D. Wang, S. Wu, et al., J. Mater. Chem. A 8 (2020) 25425–25430.
[50] K. Wu, H. Zhu, T. Lian, Acc. Chem. Res. 48 (2015) 851–859.
[51] P. Roy, G. Bressan, J. Gretton, A.N. Cammidge, S.R. Meech, Angew. Chem. Int. Ed. 60 (2021) 10568–10572.
[52] K.L. Corp, C.W. Schlenker, J. Am. Chem. Soc. 139 (2017) 7904–7912.
[53] J. Liu, P. Wang, J. Fan, H. Yu, J. Yu, ACS Sustain. Chem. Eng. 9 (2021) 3828–3837.
[54] Y. Li, Q. Zhao, Y. Zhang, et al., Appl. Catal. B: Environ. 300 (2022) 120763.
[55] Y. Li, X. Wang, Y. Hao, et al., Chin. J. Catal. 42 (2021) 1040–1050.
[56] F. Chen, W. Luo, Y. Mo, H. Yu, B. Cheng, Appl. Surf. Sci. 430 (2018) 448–456.